

Prospects for Diffractive Physics with the CDF Forward Detectors at the Tevatron

Michele Gallinaro^{1,2}

(CDF Collaboration)
The Rockefeller University
1230 York Avenue, New York, NY 10021 - USA

Abstract. The Forward Detector upgrade project at CDF is designed to enhance the capabilities for studies of diffractive physics at the Tevatron during Run II. Studies of hard diffraction and very forward physics are some of the topics that can be addressed in the next few years at the Tevatron. The program for diffractive physics, including the detectors and their commissioning, is discussed here. All the detectors have been installed and are presently collecting data.

I INTRODUCTION

During Run I, which started in 1992 and lasted until the end of 1995, the CDF experiment collected a large data sample which has been extensively studied. Considerable knowledge on diffractive physics phenomena was gained using those data (see refs. [1]– [11]).

Run II at the Tevatron Collider started in the spring of 2001. Protons and antiprotons are colliding at an energy of $\sqrt{s} = 1.96$ TeV. In preparation for Run II, improvements were made to the accelerator with the goal of achieving instantaneous luminosities of $\mathcal{L} \approx 5 \cdot 10^{32} \text{cm}^{-2} \text{sec}^{-1}$. Although the size of the data sample delivered up to now is still well below the expectations, the Tevatron will hopefully soon reach the design luminosity goal. Both the CDF and the DØ experiments underwent major upgrade projects to improve their detector capabilities. The Forward Detector upgrade project at CDF will enhance the sensitivity for hard diffraction and very forward physics.

The signature of a typical diffractive event in $p\bar{p}$ collisions is characterized by a leading proton or anti-proton and/or a region at large pseudorapidity with no particles, also known as *gap* region (Fig. 1). In order to detect such events, forward regions in pseudorapidity are extremely important.

¹⁾ Email: michgall@fnal.gov

²⁾ Presented at “LISHEP 2002 - Session C: Workshop on Diffractive Physics”, February 4-8 2002, Rio de Janeiro - RJ - Brazil.

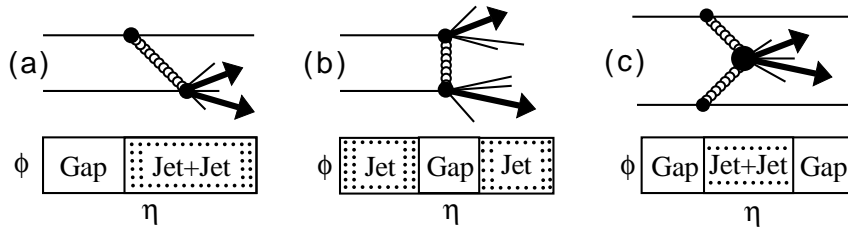


FIGURE 1. Dijet production diagrams and event topologies for (a) single diffraction, (b) double diffraction, and (c) double Pomeron exchange.

The Forward Detector upgrade project includes the *Roman Pot* (RP) fiber tracker detectors to detect leading antiprotons, a set of *Beam Shower Counters* (BSCs) installed around the beam-pipe at three (four) locations along the $p(\bar{p})$ direction to tag rapidity gaps at $5.5 < |\eta| < 7.5$, and two forward *MiniPlug* (MP) calorimeters to cover the pseudorapidity region $3.6 < |\eta| < 5.1$.

All of the above detectors have been installed and are now fully integrated with the rest of the CDF detector.

II DIFFRACTIVE PHYSICS DURING RUN II

Diffraction physics can be studied at the Tevatron Collider using the Forward Detectors. The physics topics to be addressed include studies of soft and hard diffraction, searches for centauros and disoriented chiral condensates, and forward jet production. The latter can probe both small- x and large- x regions of the proton structure function.

A Hard Single Diffraction

Hard diffraction processes are hadronic interactions which incorporate a high transverse momentum partonic scattering while carrying the characteristic signature of diffraction, namely leading p or \bar{p} particles and/or rapidity gap regions.

Hard Single Diffraction (SD) studies can be used to determine the structure of the pomeron, as well as to determine the dependence of the cross section on the recoil (anti)proton fractional momentum loss (ξ) and on the four-momentum transfer squared (t). The wide ξ coverage (down to $\xi_{\min}=0.03$) will allow the measurement of the dijet cross section as a function of ξ and thereby the determination of the pomeron contribution to the cross section and the factorization properties of hard diffraction as a function of ξ .

B Double Diffraction

The $\Delta\eta$ dependence of the ratio of dijet events with a rapidity gap between jets to non-gap events probes the coupling of the exchanged color-singlet object to quarks and gluons relative to the coupling of the normal color-octet exchange.

The MP can be used to study *soft* Double Diffraction (DD) where both proton and anti-proton dissociate. This process, which is characterized by a rapidity gap between two clusters of particles in the regions of large (positive and negative) pseudorapidity, has been studied in Run I [4]. The MP will allow the measurement to be extended to larger gaps. The ratio of DD to *minimum bias* events may shed light on the mechanism of the survival probability of the rapidity gap in events with jets.

C Double Pomeron Exchange

This is an area of great interest for hard diffraction processes. In Run I, only a small number of Double Pomeron Exchange (DPE) dijet events were observed using a combination of an anti-proton tag on the west side and a rapidity gap tag on the opposite (east) side [5].

During Run II, the momentum of the pomeron associated with the gap can be measured by the segmented MP calorimeter (by measuring the center-of-mass energy of the pomeron-pomeron system using calorimeter information). Low mass exclusive DPE events (events with rapidity gaps on both sides) can be searched for by using both the Plug and the MP calorimeters. Furthermore, the exclusive dijet and $b\bar{b}$ production cross sections can also be measured. The latter is of much interest to diffractive Higgs production [13], as recent studies [14] indicate that Higgs boson and dijet production via DPE may be non-negligible at the Tevatron.

D Forward Jet Production

The Bjorken scaling variable (x) can be studied, both in the small- x and the large- x regions of the proton structure function, by measuring the cross section of events with two jets in the forward regions. The dijet events probe the parton density and do not discriminate between gluons and quarks. Small- x values can be studied using Same Side (SS) dijet events, while large- x regions can be explored with both SS or opposite-side (OS) dijet events. The large- x gluon density of the proton can be probed in events with a prompt (isolated) photon in the central region and a forward jet in the MP.

E Centauros and Disoriented Chiral Condensates

The unique signature for Centauro or Disoriented Chiral Condensates (DCC) events is a high multiplicity of relatively low P_T clusters of particles depositing predomi-

nantly hadronic or electromagnetic energy. Such particles have been searched for in Run IA data [12] with negative results. The fine segmentation of the MP and the excellent position resolution, not only for leptons and photons but also for hadrons, makes the MP an ideal detector for searching for Centauro and DCC events.

III DETECTORS

Theories and expectations cannot be proven, right or wrong, without experiments. Experiments need detectors. The detectors built and installed at CDF during the preparation for Run II with the aim of addressing the above topics are described in the following sections.

A Roman Pot Fiber Tracker

The pomeron structure can be determined by using the kinematic variables in diffractive dijet events, provided that the momentum of the pomeron is known. During Run I, the pomeron momentum was determined using the RP to measure the momentum of the leading anti-proton.

The RP is a fiber detector spectrometer with a 2-meter lever arm located approximately 57 meters from the *Interaction Point* (IP) downstream of the anti-proton (Fig. 2). The RP detector consists of three stations, approximately one meter apart from each other (Fig. 3). Each station consists of one trigger counter and one

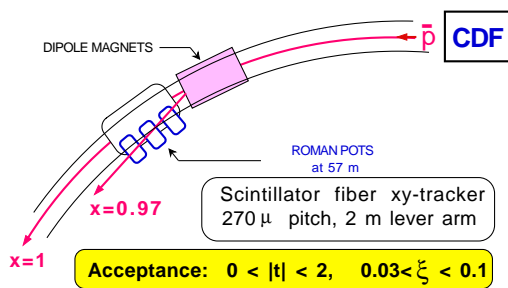


FIGURE 2. Schematic view of the Roman Pot spectrometer at the Tevatron.

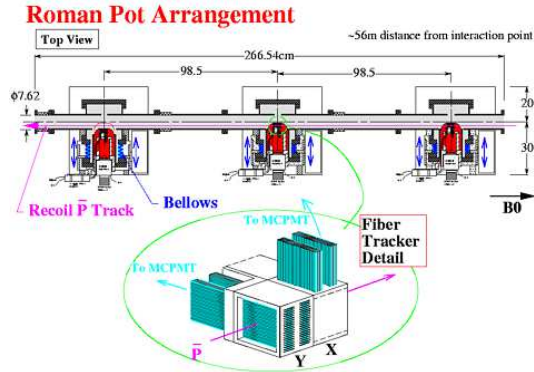


FIGURE 3. Schematic view of the Roman Pot fiber tracker detector.

80-channel scintillation fiber detector viewed by a Hamamatsu H5828 80-channel Photo-Multiplier Tube (PMT). The fiber detector reads X (40 channels) and Y (40 channels) coordinates to identify the position of the tracks with a resolution of approximately $100 \mu\text{m}$.

In preparation for Run II, the detector was reinstalled as in Run I. In contrast, the read out electronics was completely redesigned to take into account the shorter (with respect to Run I) 396 nsec spacing between bunches. Moreover, the beam polarity at the RP location was reversed with respect to Run I, and the anti-proton beam travels now closer to the RP detector. This will allow close to full acceptance down to $\xi \sim 0.03$ (in Run I the region of full acceptance was $0.05 < \xi < 0.1$). Lower values of ξ are necessary to enhance the rate of diffractive events. A coincidence signal of the three counters selects events with an outgoing anti-proton at the RP location and is used as an input at Level 1 trigger. This coincidence signal is used together with other signatures in the CDF detector to enhance the selection of diffractive events.

B Beam Shower Counters

SD and DPE processes are characterized by forward rapidity gaps. An ideal rapidity gap tagger at the trigger level would only select these events and can be accomplished with a set of scintillation counters around the beam-pipe at several locations along the p and \bar{p} directions covering the forward pseudorapidity region. The BSCs can be used to identify diffractive events with a leading anti-proton, or also to veto non-diffractive minimum bias events. This is important for the inclusive RP and DPE triggers.

The BSCs detect particles traveling in either direction from the IP along and near the beam-pipe and cover the pseudorapidity region $5.5 < |\eta| < 7.5$. There are four BSC stations on the west side and three on the east side of the IP. All stations are located along the beam-pipe, at increasing distances from the IP as one goes from BSC-1 to BSC-4 (Fig. 4). BSC-1, 2 and 3 consist of two stations each, positioned symmetrically with respect to the IP, whereas BSC-4 consists of a single station on the west side.

Stations are made of two scintillation counters, except for the BSC-1 stations, which have four counters. Since each counter is connected to its own PMT, the entire system consists of 18 signal channels, 10 from the west and 8 from the east side.

The output signals from the PMTs on each side of the IP identify tracks traveling close to the beam-pipe. BSCs separately provide East and West *gap* triggers at Level 1, when no signal is observed in either counter. Trigger rates are satisfactorily within $\approx 10\%$ from Monte Carlo expectations (Fig. 5) at different values of luminosity. *Gap* triggers are then combined with other triggers at Level 2 and at Level 3 in order to provide a purer diffractive event sample.

The BSC-1 counters can also be used to monitor Tevatron beam losses and collision rates, as well as the x - y beam position.

The signals from BSC-1 are referred to as “Out-of-Time” for particles hitting the counters ~ 20 nsec before interaction time (also due to beam losses), and as “In-Time” for particles coming from a collision and hitting the counters ~ 20 nsec

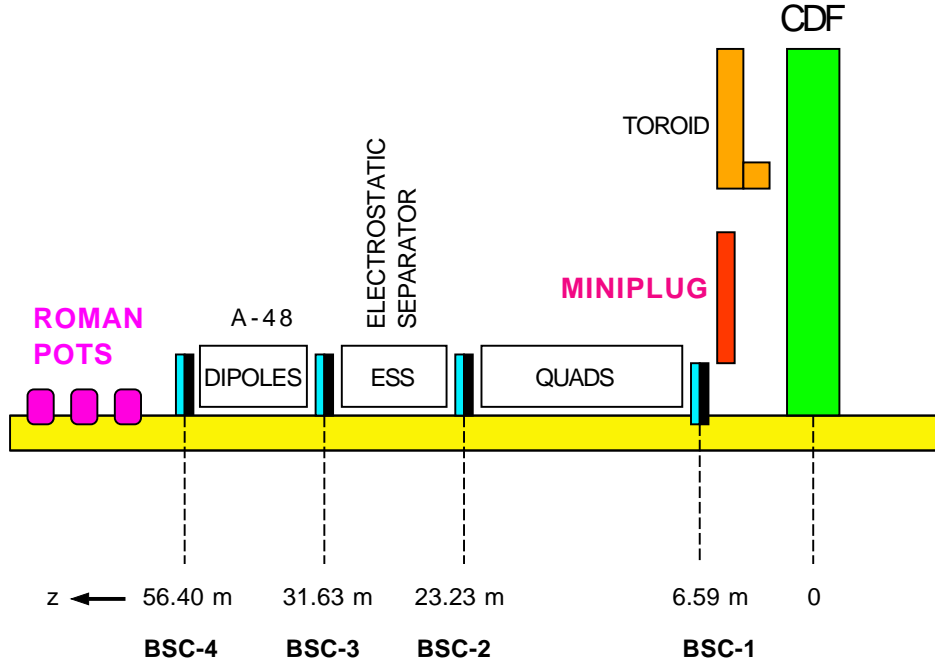


FIGURE 4. Location of the Forward Detectors along the \bar{p} direction on the West side of the CDF central detector (not to scale). On the East side, only the first three BSC stations are installed, as there is no room for BSC-4.

after interaction time (collision rate and diffractive physics measurements). The *East-West* coincidence trigger requires at least one BSC-1 counter on each side of the interaction to fire within a 20 nsec window centered on the beam crossing time. The luminosity \mathcal{L} can be calculated from the collision rate using the formula:

$$N[Hz] = \mathcal{L}[Hz/mb] \cdot \sigma[mb] \cdot \epsilon,$$

where σ is the $p\bar{p}$ cross section and ϵ is the acceptance of the counters. The beam-beam cross section for the $E \cdot W$ coincidence is calculated to be $\sigma_{E \cdot W} = \sigma \times \epsilon = 25.6$ mb. The coincidence rate between BSC-1 East and BSC-1 West is shown in Figure 6 and is compared to the measurement by the Čerenkov Luminosity Counter (CLC).

The BSC-1 counters are segmented in four quadrants in ϕ , around the beam-pipe. The ϕ segmentation allows real-time monitoring of the x - y position of the beam. The information can be used by the Accelerator Beams' Division to steer the beam in the center of the CDF detector.

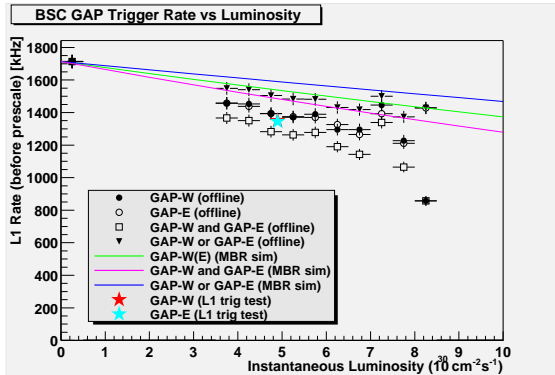


FIGURE 5. Level 1 *gap* trigger rates provided by the BSCs at different values of the luminosity.

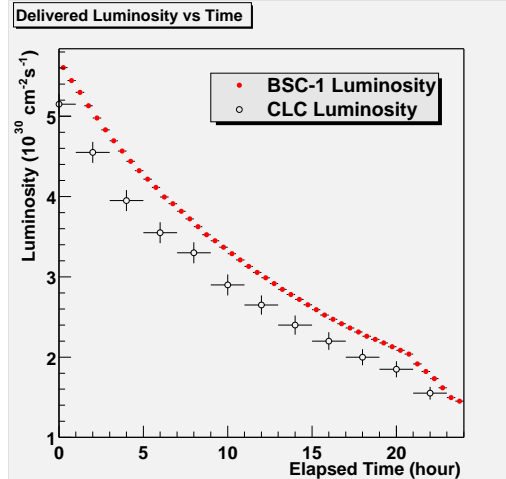


FIGURE 6. The *East-West* coincidence rate from BSC-1 is compared with the measurement provided by the Čerenkov Luminosity Counters.

C MiniPlug Calorimeters

The program of hard diffraction and very forward physics for Run II benefits from two forward MP calorimeters in the pseudorapidity region $3.6 < |\eta| < 5.1$ designed to measure the energy and lateral position of both electromagnetic and hadronic showers. The MPs approximately double the pseudorapidity region covered by the Plug calorimeters, which is $1.1 < |\eta| < 3.5$. The MP and the Plug calorimeters can measure the width of the rapidity gap(s) produced in diffractive processes and will allow extending the Run I studies of the diffractive structure function to much lower values of the fractions ξ , where ξ is the momentum of the proton carried by the Pomeron. The low ξ values can be measured from the size of the rapidity gap region using information from both BSCs and MPs.

The MPs consist of alternating layers of lead plates and liquid scintillator read out by wavelength shifting (WLS) fibers. The WLS fibers are perpendicular to the lead plates and parallel to the proton/anti-proton beams in a geometry where *Towers* are formed by combining the desired numbers of fibers and read out by Multi-Channel PhotoMultipliers (MCPMTs).

Each MP is housed in a cylindrical steel barrel 26" in diameter and has a 5"-hole concentric with the cylinder axis to accommodate the beam-pipe (Fig. 7). The active depth of each MP is 32 radiation lengths and 1.3 interaction lengths.

The tower geometry is organized in three concentric circles around the beam-pipe (Fig. 8) with an *inner*, a *middle* and an *outer* ring. Each ring covers a different region in pseudorapidity. This allows triggering on different η regions, both for events with a *gap* region and for events with high- E_T clusters.

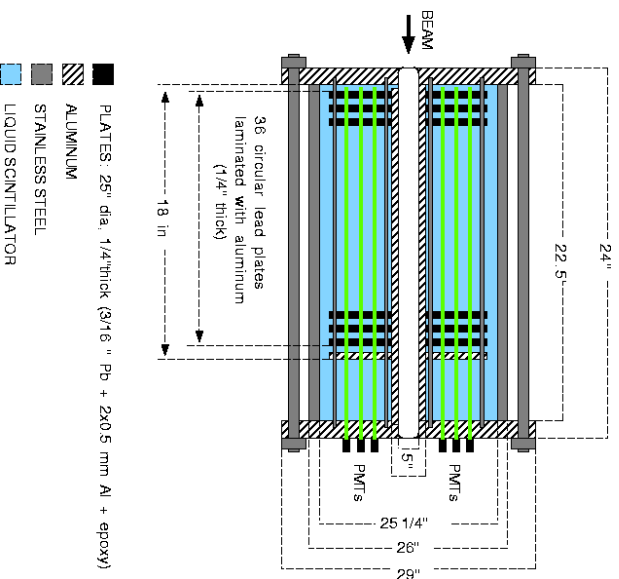


FIGURE 7. Schematic side view of a Mini-Plug (not to scale).

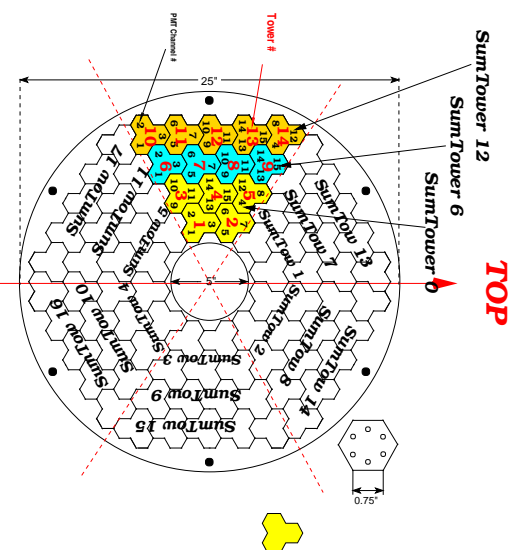


FIGURE 8. Tower geometry of the East Miniplug calorimeter (viewed from the interaction point).

East Miniplug (viewed from IP)

The design is based on a hexagon geometry. Uniformly distributed over each plate, holes are conceptually grouped in hexagons and each hexagon has six holes. A WLS fiber is inserted in each hole. The six fibers of one hexagon are grouped together and are viewed by one MCPMT channel. The MCPMT outputs are added in groups of three to form 84 calorimeter towers. The entire MCPMT can also be read out through the last dynode output, indicated as *Sum-Tower* in Figure 8, and provides triggering information. Each MP has a total of 18 *Sum-Tower* signals, divided in three rings.

An additional clear fiber carries the light from a calibration LED to each MCPMT pixel. The LED allows a first relative gain calibration to equalize the MCPMT from each ring. It also allows periodical monitoring of the MCPMT response. A cross-calibration between data and Monte Carlo expectations allows an absolute energy calibration.

Cosmic ray muons were used to test one 60° wedge of the East MP. In this test, the cosmic ray trigger fired on a 2-fold coincidence of the scintillation counter paddles located on top and on the bottom of the MP vessel, placed with the towers pointing upward. The outputs from Towers #6, 7, 8 and 9 and from *Sum-Towers* #2, 8 and 14 (Fig. 8) were read out. An energy isolation cut selects only those muons which went through the entire length of the central *Sum-Tower* (#8) and vetoed

on the signals from the neighboring Sum-Towers (#2 and 14). The single photoelectron response for Sum-Tower #8 is measured using a signal from a ^{60}Co source randomly gated (Fig. 9). The single tower response to a *minimum ionizing particle* is estimated to be approximately 120 photoelectrons, exceeding the design specification.

The MPs have been installed along the beam-pipe within the hole of the muon toroids at a distance of 5.8 meters from the center of the detector (Fig. 10).

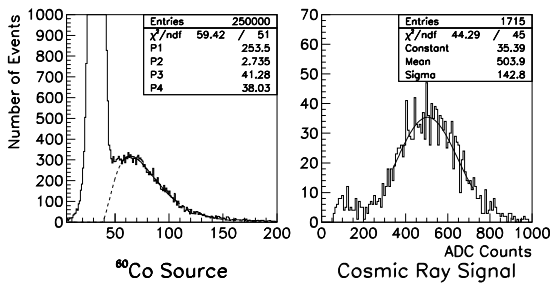


FIGURE 9. Cosmic ray test for *Tower* #7 on East MiniPlug: ^{60}Co source signals (left). The parameter $P3$ corresponds to the pulse height of a single photoelectron; cosmic ray spectrum after an isolation requirement is fitted to a Gaussian distribution (right).

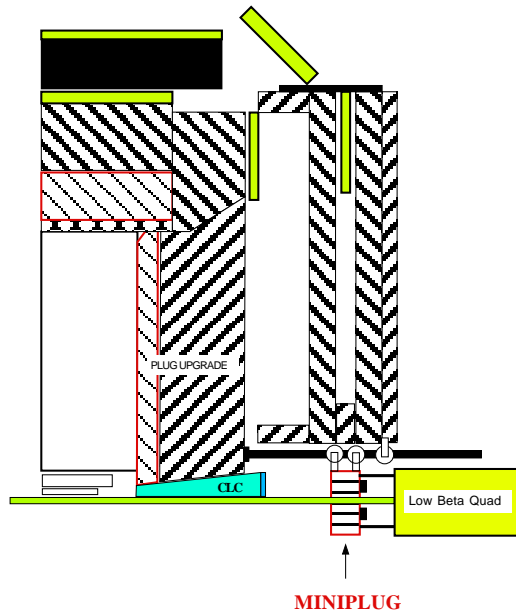


FIGURE 10. Schematic drawing of a quarter view of the CDF detector showing a MiniPlug calorimeter installed inside the toroids (not to scale).

IV DIFFRACTIVE TRIGGERS

The triggers for diffractive physics are needed to enhance the selection of the diffractive events. All of the Forward Detectors provide triggering information to the *Level 1* trigger selection, which is then combined together with other physical entities from the rest of the CDF central detector such as, for example, large transverse energy *jets*. The events selected by the diffractive triggers are then written on disk at a rate of approximately 2 Hz.

V CONCLUSIONS AND PROSPECTS

The program for diffractive physics during Run II at the Tevatron includes studies of hard diffraction and of double Pomeron exchange. Some of these topics and desired goals for the immediate future have been discussed here.

In addition to other sub-detector parts, the CDF experiment is preparing for the next few years of data-taking with a detector that has been exceptionally improved in many areas. The Forward Detector upgrade project is essential for the program of diffractive physics studies. The detectors have been installed, the commissioning is well underway, and some of the results have been presented here. The Forward Detectors are getting ready to take good quality physics data as the Tevatron is reaching its design goals for luminosity.

These data will hopefully answer some of the questions addressed here and allow a better understanding of phenomena in hard diffraction and very forward physics at the Tevatron in $p\bar{p}$ collisions.

In conclusion, Run II is finally becoming a reality after many years of detailed studies, accurate designs, promising improvements and intense upgrading.

VI ACKNOWLEDGMENTS

My warm thanks to the organizers of this conference for a wonderful workshop, and to all the people who strenuously contributed to this multi-year project.

REFERENCES

1. K. Hatakeyama: these proceedings.
2. “Diffractive Dijet Production at $\sqrt{s} = 630$ and 1800 GeV at the Fermilab Tevatron”, D. Acosta *et al.* (CDF Collaboration), *Phys. Rev. Lett.* *88* (2002) 151802.
3. “Observation of Diffractive J/ψ Production at the Fermilab Tevatron”, T. Affolder *et al.* (CDF Collaboration), *Phys. Rev. Lett.* *87* (2001) 241802.
4. “Double Diffraction Dissociation at the Fermilab Tevatron Collider”, T. Affolder *et al.* (CDF Collaboration), *Phys. Rev. Lett.* *87* (2001) 141802.
5. “Dijet Production by Double Pomeron Exchange at the Fermilab Tevatron”, T. Affolder *et al.* (CDF Collaboration), *Phys. Rev. Lett.* *85* (2000) 4215.
6. “Diffractive Dijets with a Leading Antiproton in $p\bar{p}$ Collisions at $\sqrt{s} = 1800$ GeV”, T. Affolder *et al.* (CDF Collaboration), *Phys. Rev. Lett.* *84* (2000) 5043.
7. “Observation of Diffractive b -quark Production at the Fermilab Tevatron”, T. Affolder *et al.* (CDF Collaboration), *Phys. Rev. Lett.* *84* (2000) 232.
8. “Events with a Rapidity Gap between Jets in $p\bar{p}$ Collisions at $\sqrt{s} = 630$ GeV”, F. Abe *et al.* (CDF Collaboration), *Phys. Rev. Lett.* *81* (1998) 5278.
9. “Dijet Production by Color-Singlet Exchange at the Fermilab Tevatron”, F. Abe *et al.* (CDF Collaboration), *Phys. Rev. Lett.* *80* (1998) 1156.

10. “Measurement of Diffractive Dijet Production at the Fermilab Tevatron”,
F. Abe *et al.* (CDF Collaboration), *Phys. Rev. Lett.* *79* (1997) 2636.
11. “Observation of Diffractive W-Boson Production at the Fermilab Tevatron”,
F. Abe *et al.* (CDF Collaboration), *Phys. Rev. Lett.* *78* (1997) 2698.
12. P. Melese, “Search for Centauro events at CDF”,
IX “Hadrons in Collision” Workshop (PBARP96), Padova, Italy, May 1996.
13. A. Rostovtsev: these proceedings.
See also: M. Albrow and A. Rostovtsev, *hep-ph/0009336*.
14. M. Boonekamp, R. Peschanski, C. Royon,
“Inclusive Higgs Boson and Dijet Production via Double Pomeron Exchange”,
Phys. Rev. Lett. *87* (2001) 251806.